

**Deformation, metamorphism and exhumation –
quantitative models for a continental collision zone
in the Variscides**

M. Seyferth and A. Henk

Institut für Geologie, Universität Würzburg

Pleicherwall 1, D-97070 Würzburg,

Germany

Phone: +49-(0)-931-312695

Fax: +49- (0)-931-312378

e-mail: michael.seyferth@mail.uni-wuerzburg.de

Word count

abstract:	155
text:	5454
references:	862
tables:	263
figure captions:	471

Abbreviated title

FE Models on a Variscan Collision Zone

Abstract: Two-dimensional thermo-mechanical finite-element models are used to gain a quantitative insight into the complex strain partitioning in continental collision zones. If model with Moho temperatures of 700 – 900 °C, as is indicated by petrological data, are simulated, frequently-used flow laws for the lower crust cannot reproduce significant crustal thickening. Instead decoupling between crust and mantle occurs, resulting in the widening of a diffuse deformation zone. To reproduce observed petrological data and orogen geometries, a stronger lower crust, with viscosities between 10^{21} – 10^{23} Pas, is required. Models are applied specifically to a collision zone from the Variscan Orogen of Central Europe to understand the tectonometamorphic history, strain partitioning within the collision zone, as well as the rapid syn-convergent exhumation of metamorphic complexes. Model predictions agree with the observed distribution of peak metamorphic conditions and show systematic variations of contemporaneous pressure-temperature (P-T) paths across the collision zone.

Rocks in continental collision zones may experience burial, intense deformation and metamorphism. But the collision of continental crust does not only bring rocks to greater depths and temperatures. It also provides a very effective mechanism to bring them back to the surface. In general, two processes can contribute to the exhumation of rocks in orogenic settings: surface erosion and tectonic denudation by normal faulting and ductile thinning (England & Molnar 1990; Jamieson 1991). Both exhumation processes are related to the topography generated by the continent-continent collision. The topographic relief of an orogen does not only enhance exhumation by erosion of the overburden. Additionally, local gravitational instabilities induced by the high topography and over-thickened crust can result in exhumation by syn-convergent extension (Dewey 1988; Burg *et al.* 1994). The latter mechanism implies a pronounced strain partitioning within the colliding continental crust as its lower parts are still under compression, while its uppermost part may already be extending. The concept of strain partitioning is used in the sense to describe how strain varies both laterally and vertically in the modelled two-dimensional section. Numerical models have proven to be a particularly valuable tool in gaining a quantitative understanding of the fundamental processes controlling the evolution and structure of orogenic belts (e.g., Willett *et al.* 1993; Beaumont *et al.* 1994). In particular, they provide information on how strain is distributed within a collision zone and help to assess to what extent the deformation commonly observed in upper and middle crustal rocks can be used as an indicator for the tectonic processes in the deeper crust and upper mantle.

In this study we use finite-element techniques to get a quantitative insight into the temporal and spatial distribution of deformation and metamorphism, as well as the mechanisms for rapid syn-convergent exhumation in areas of colliding, hot continental crust. We compare the model predictions with field data from a well-documented collision zone located at the northern flank of the Late Palaeozoic Variscan Orogen in Central Europe. Available data sets relevant to the orogenic evolution of this area include petrological and

geochronologic data (e.g., Okrusch 1995), seismic sections (Meissner & Bortfeld 1990) and convergence estimates (Oncken 1998). Although fossil orogens usually lack some information such as paleo-topography and erosion rates, they can provide insights into deeper crustal levels and the processes of their exhumation to the surface. In addition, they can provide information on the complete orogenic history rather than being restricted to early stages of orogenesis observable in active orogens. Thus, our modelling results may have general implications for the understanding of strain partitioning, metamorphism and exhumation processes in continental collision zones characterized by elevated crustal temperatures.

Modelling concept

Methodically, this study builds on the work of Willett *et al.* (1993) and Beaumont and Quinlan (1994), among others, who used two-dimensional finite-element models to calculate crustal deformation within compressional orogens and compared model predictions with natural examples. The numerical simulations describe collision of two continental fragments by applying displacements to material points at the base of one crustal block, while the base of the other is fixed horizontally (Fig. 1). The point, where the discontinuity in the basal boundary condition occurs is termed S and represents the locus of asymmetric detachment and underthrusting of the mantle lithosphere. As a result of convergence, an orogen develops showing a marked asymmetry in the general topographic relief, as well as in the internal structure and strain distribution. Typically, the collision zone is characterized by a broad zone of thrusts and folds verging toward the subducting plate, the so-called pro-side, while a narrower zone of deformation verging towards the stationary plate forms on the retro-side. Deformation also follows a typical temporal sequence starting with an initial stage of block uplift between two conjugate deformation zones termed step-up shears which ultimately leads

to a pro-wedge with minimum critical taper and a retro-wedge comprising two segments with a maximum and minimum critical taper (Fig. 1; terminology after Willett *et al.* 1993). This basic deformation pattern can be modified by external processes, i.e. asymmetric erosion, as well as thermal weakening of the thickened crust which leads to plateau formation and gravitational collapse (Willett *et al.* 1993). Beaumont *et al.* (1994), Beaumont and Quinlan (1994) and Jamieson *et al.* (1998) give comprehensive discussions of the modelling concept and variations in input parameters, e.g. temperature gradient, rheological stratification, locus of the discontinuity in the prescribed displacement field and erosional denudation. It should be noted that the models presented in these papers assume very low to moderate crustal temperatures, i.e. Moho temperatures between 360 and 600°C. Temperatures in the Variscides were significantly higher, which is fundamental in understanding the evolution of this orogen. Thus, prior to applying the model concept outlined above to the specific continental collision zone of the Variscan Orogen, we will briefly discuss the special features of our numerical modelling approach and some general implications of high crustal temperatures and weak rheologies on the resulting orogen geometry and strain distribution.

Numerical modelling approach

The numerical simulations are based on a two-dimensional plane-strain finite-element approach using the ANSYS[?] (ANSYS Inc., Houston, USA) software package. A comprehensive description of the capabilities of ANSYS[?] for the numerical simulation of geodynamic processes is given by Henk (1998). The model in this study describes a crustal-scale section oriented perpendicular to the strike of the evolving orogen. The crust is divided into an upper and a lower part, each characterized by specific thermal and mechanical material properties (Tab. 1). The thermal calculations consider - among others - temperature-dependent thermal conductivities and radiogenic heat production. Thermal boundary conditions of the model are a constant heat flow applied to the base of the crust and a constant

surface temperature of 0°C. Lateral variations in the basal heat flow which may result from mantle subduction (Jamieson *et al.* 1998) and the preceding oceanic subduction stage are not considered. For the mechanical calculations the irreversible deformation in the brittle domain is described by an elastic-perfectly plastic material law with a pressure-dependent yield strength approximating Byerlee's relationship (Byerlee 1978) and assuming hydrostatic fluid pressure conditions. Deformation in the ductile domain can be described either by temperature-dependent viscous flow or by temperature- and strain-rate-dependent creep laws (see below). The top of the model is a free surface and isostatic forces act at its base. Convergence is modeled by a displacement boundary condition applied to the basal nodes left of a point S. This model concept implies that convergence is driven by the mantle lithosphere until it detaches at the mantle subduction point S. As the crustal rheology is strongly temperature-dependent and substantial advective heat transport occurs, the thermal and mechanical calculations have to be coupled via temperatures and displacements (see Henk 1998 for further details on the modelling techniques).

High crustal temperatures and/or convergence in excess of 100 km can result in severe distortion of the basal elements and often cause numerical problems. In order to overcome these limitations a remeshing algorithm was developed as an add-on to ANSYS[?]. With this technique the deformed finite-element grid can be repeatedly replaced by a new one which is capable to experience further deformation. The new grid consists of the same number of elements and covers the geometry of the previously deformed model. It also keeps track of the material domains of the upper and lower crust. New nodes are arranged in vertical columns, thus approaching nearly rectangular element shapes.

The modelling results calculated prior to remeshing (temperature, strain) are interpolated to the new finite-element grid. To keep track of the evolution experienced by the initial grid points, a tracking grid of marker points is used. This grid describes the particle paths in space and time and can be directly compared to observed P-T-t paths. Since four-

node elements are used, the relative position of marker points can be described by three parameters, comprising the number of the element currently containing the marker point and the marker points position relative to opposite element faces. Vice versa, the absolute marker point position is updated using the position of the corresponding edge nodes.

This technique not only permits large as well as localized deformation, but also allows changes in the domain geometry by adding or removing parts of the model. Thus, it is possible to describe sedimentation and erosion at the upper surface of the model as well as processes such as tectonic erosion and delamination at the base of the crust.

Impact of temperature and rheology on the orogen geometry and strain distribution

Crustal temperature and rheology are the two most important factors controlling the deformation within an evolving orogen, as well as its overall shape. Both factors are coupled since the rheology in the ductile domain is strongly temperature-dependent. High temperatures and the corresponding low integrated strength of the crust may impose important limitations on the development of significant crustal thickness and topography within continental collision zones. This relationship between rheology and orogen geometry can be illustrated by two numerical experiments which differ only in the assumed initial temperature field (Fig. 2). Both models apply the power-law creep parameters for dry anorthosite (Shelton & Tullis 1981), commonly used in geodynamic studies to represent the lower crust. After 100 km of convergence, the “cold” model, i.e. with initial Moho temperatures of 500 °C, shows a localized crustal thickness increase by up to 55%. The strain distribution depicts the typical bivergent pattern rooting at point S with additional subhorizontal strain zones between upper and lower crust (Fig. 2a; see also Beaumont and Quinlan 1994, their figures 2 and 11). The comparatively high strength of the lower crust and the resulting good coupling between crust and mantle are responsible for the strain localization and crustal thickening in the vicinity of S. In contrast, the same model scenario but with an initial Moho temperature of 700 °C shows

no such strain localization but only a wide zone of diffuse deformation (Fig. 2b; see also Beaumont and Quinlan 1994, their figure 6). The crust is only thickened by 25% indicating that crustal convergence is compensated by widening of the deformation zone rather than crustal thickening. Any asymmetry in orogen geometry and strain distribution is only very weakly developed. The reason for this is the low strength, particularly of the lower crust, so that the imposed movement of the mantle is only weakly coupled to the deformation within the crust. Consequently, a Moho-parallel high-strain zone develops in the lowermost crust spreading out towards the pro- and retro-side.

From these modelling results it appears very difficult to thicken hot continental crust to generate sufficient topography which would encourage substantial synconvergent exhumation by erosion and tectonic denudation. Obviously, such a conclusion would be in contradiction with field observations from several orogens including the Variscan Orogen of Central Europe which show focused deformation and crustal thickening although petrological data point to lower crustal temperatures of 800 °C and more. Also numerical models assuming a wide zone of weak, hot model crust, embedded between stronger and colder crust ('vise models', see Ellis et al., 1998) result in diffuse deformation and only minor crustal thickening. This inconsistency could be solved by recent experimental studies which indicate that the effective strength of rocks, representative for the lower crust, may be much higher than previously thought (Mackwell *et al.* 1998; Vauchez *et al.* 1998). Inappropriate sample preparation may have changed the rheologies of supposed dry rocks, which were actually softened by water weakening, breakdown of hydrous minerals and/or dehydration melting (Mackwell *et al.* 1998). The revised flow laws would imply that the lower crust is much stronger and may be as stiff as the upper mantle. Consequently, a good mechanical coupling between lower crust and mantle would exist at the Moho allowing localized deformation and crustal thickening. Additionally, the discrepancy between laboratory measurements and large-

scale behaviour of the lower crust may in part be due to sample size and extrapolation of strain rates over several order of magnitude (Kohlstedt *et al.* 1995).

The present study utilizes the flow laws for dry Westerly granite (Hansen & Carter 1983) and dry Maryland diabase (Mackwell *et al.* 1998) to represent upper crust and lower crust, respectively (Fig. 3). However, even these dry rheologies exhibit a strong strain-rate dependence and due to the imposed displacement boundary condition a high-strain zone develops at the base of the crust. Although these effects of strain softening and decoupling between crust and mantle, respectively, are less pronounced than for the wet rheologies, they still impede localized crustal thickening. If this strain rate dependence of the power-law rheology is removed by assuming an average strain rate of 10^{-14} s^{-1} , effective viscosities between 10^{21} and 10^{23} Pa s , depending on temperature, result for the lower crust (Fig. 3). If such a temperature-dependent viscous rheology is applied to the model scenario outlined above the resulting numerical model shows a pronounced thickness increase and localized strain accumulation in spite of high crustal temperatures (Fig. 2c).

Case study: strain partitioning and rapid syn-convergent exhumation at the boundary between internal and external zone of the Variscan Orogen

The Variscan Orogen in Central Europe was formed by the sequential collision of microplates, derived from the northern margin of Gondwana, with Laurentia and Baltica during the Carboniferous (see Franke 1992; Oncken 1997; Walter 1992 and this volume for comprehensive reviews of the Variscan evolution and regional geology, respectively). Typical features of the final collision stage are the widespread and almost synchronous HT-LP metamorphism and granite magmatism as well as the rapid exhumation of metamorphic complexes. This case study concentrates on a cross-section through the northern flank of the

Late Palaeozoic Variscan Orogen and aims for a quantitative analysis of the collision between a passive margin (Renohercynian Zone) in the north and a former magmatic arc situated on a fragment of continental crust (Mid German Crystalline Rise and Saxothuringian Zone) in the south. This collision zone also represents the boundary between the internal zone of the orogen and the external fold-and-thrust belt. This area was chosen because various data sets are available to constrain a numerical modelling approach, e.g., estimates for convergence velocity, crustal shortening (Oncken 1998), petrological and geochronologic data (for comprehension see Okrusch 1995). Additionally, deep seismic profiles (Meissner & Bortfeld 1990) can be used to infer the internal structure of the collision zone and the location of high-strain zones within the crust.

Geological constraints for numerical model

The collision zone between the Renohercynian and Saxothuringian Zone traces the former site of the Lizard-Giessen-Harz Ocean, a relatively small oceanic basin presumably only a few hundred kilometers wide (Franke 1992; Oncken 1997). Closure of this basin from the late Middle Devonian onwards resulted in the formation of a magmatic arc in the northern Saxothuringian zone, the so-called Mid German Crystalline Rise (MGCR). Subduction of oceanic crust was essentially completed by the end of the Devonian. Continent-continent collision and final closure of the basin continued throughout the Early Carboniferous and probably accelerated from the Late Viséan onwards. Continental collision between the Renohercynian and Saxothuringian zones was contemporaneous with rapid exhumation of metamorphic rocks as is indicated by thermal-kinematic modelling of various P-T-t data sets from the MGCR (Henk 1995). At approximately 325 Ma, the MGCR was thrust above the southernmost Renohercynian zone and subsequently the deformation front continued to migrate further northwestward. The youngest sediments which were affected by compression

are located in the Ruhr Basin area and are Westphalian D (about 305 Ma) in age (Ziegler 1990).

Within the Rhenohercynian Zone, the rocks presently exposed at the Earth's surface are unmetamorphosed near the orogenic front, but peak metamorphic pressure conditions gradually increase towards the south and reach up to 6 kbar in the southernmost part (Northern Phyllite Zone; Anderle *et al.* 1990). Crustal shortening across this orogenic wedge was achieved mainly by thrusting and amounts to 42 % (Dittmar *et al.* 1994), i.e. 116 km assuming a present width of 160 km. North-verging thrusts separate the Rhenohercynian Zone from the crystalline core of the Variscides. The MGCR represents a roughly triangular block bounded by outward-verging thrusts (Oncken 1998). Rocks at the surface show amphibolite-facies metamorphic grade with peak pressures of 6 – 8 kbar at 600 – 650 °C (Willner *et al.* 1991; Okrusch 1995). Immediately south of the MGCR the northern Saxothuringian zone consists of a small south-facing fold and thrust belt, which has been interpreted as the retro wedge of the collision zone (Oncken 1998; Schäfer 1997). Shortening within this wedge is less than 40% and is achieved by folding and ductile shortening rather than thrusting. Peak metamorphic pressures increase from close to zero near the southern tip of the wedge to 4 – 5 kbar at the northern rim (Kemnitz 1995; Schäfer 1997). Compared to the pro-side, the pressure gradient on the retro-side is much steeper.

In summary, the general structure of the collision zone between the Rhenohercynian and Saxothuringian shows several features which are typical for small, bivergent orogens. The total amount of shortening across the Rhenohercynian pro-wedge, the pop-up structure of the MGCR and the Saxothuringian retro-wedge was estimated by Oncken (1998) to be at least 250 km.

Numerical model of the study area

The numerical model comprises an initially 1200km long section, which represents a traverse through the Rhenohercynian and Saxothuringian tectonometamorphic units at the onset of continental collision, i. e. after the closure of the Lizard-Giessen-Harz Ocean. The model is oriented perpendicular to the strike of the Variscan units and the large model width is necessary to avoid disturbance of the modelling results by side-wall effects. Initially, a uniform Moho depth of 26 km is assumed, averaging the crustal thicknesses estimated by Oncken (this volume) for the Rhenohercynian passive margin, the magmatic arc of the evolving MGCR and the adjacent Saxothuringian Basin. Altogether, the numerical model consists of 1960 elements.

The rheology of the upper and the lower crust is approximated by flow laws for granite and dry diabase. The assumption of dry conditions in the lower crust in the vicinity of the modelled traverse may be justified by its granulitic composition documented by xenoliths found in tertiary volcanics (Blundell *et al.* 1992).

The convergent plate boundary between the Rhenohercynian Passive Margin and the Saxothuringian Terrane is indicated by the S point at the base of the model crust, which is initially located at a distance of 700 km from the left model margin. The mechanical boundary conditions reflect southeast-directed mantle subduction and underthrusting of the left-hand plate, i.e. the Rhenohercynian zone. The convergence velocity is assumed to be 15 mm a^{-1} over a time span of 17 Ma, corresponding to a total amount of shortening of about 250 km, as was estimated by Oncken (1998) for the minimum amount of convergence.

The influence of surface processes on the deformation and exhumation pattern is taken into account by applying moderate erosion rates to the model surface. As no specific information on erosion rates exists for the Variscides, some general values published by Summerfield & Hulton (1994) have been used to establish multilinear functions describing erosion rate versus surface elevation. However, there are geological data from the study area

which provide information about the relative distribution of erosion: the metamorphic profile shows more pronounced exhumation at the northwestern flank of the orogen and syncollisional flysch sediments were transported almost entirely towards the northwestern foreland (Oncken, this volume). Both facts imply an asymmetric erosion, which was focused on the northwestern flank of the orogen, i.e. towards the pro-side. Therefore, initial model runs using a uniform erosion rate have been modified by introducing a watershed at the maximum model surface elevation and different erosion rates on either side of it. Erosion rates on the proside were assumed to be 10 times larger than on the retroside.

The deformation of the initial crustal section in response to the prescribed displacement boundary condition was studied using the dynamic finite-element approach outlined above. The time step for the mechanical and thermal calculations is 100 ka, whereas remeshing of the deformed finite-element grid is carried out every 1 Ma.

Results of the numerical simulation

Modelling results are illustrated using the tracking grid which represents the cumulative displacement of the initial grid nodes. The deformed tracking grid at the end of the convergence stage, i.e. after 17 Ma and 250 km of convergence is shown in Fig. 5a. The deformed grid of the upper plot shows a dome-like zone of uplifted lower crustal rocks, whose most prominent part is related to the retro-zone of the orogen. There is also a notable difference in the dip angles of the top of the lower crust: a more gently-dipping pro-side and a steeply-dipping retro-side.

This asymmetry is also clearly visible on finite strain plots (Fig. 5b). Strain accumulated during the orogeny is mainly focused on the material boundaries at the Moho (i.e. the model base) and between the upper and the lower crust. Both boundaries act as major zones of subhorizontal ductile shearing, but, in contrast to the low-viscosity model depicted in Fig. 2a, coupling between the upper mantle and the model crust is still effective enough to thicken the

crust by more than 50%. Due to the large amount of convergence, as well as the influence of surface erosion, the bivergent strain pattern is less prominent than in the initial stages (e.g. in Fig. 2a).

Comparison to seismic reflection profiles

The deformed finite-element grid shown in Fig. 5a represents the situation after continental collision ceased. Immediately afterwards, the thickened crust of the Variscan Orogen was extended by a combination of plate boundary stresses and gravitational forces (Henk 1997). This postconvergent crustal reequilibration occurred within a very short time span of about 20 Ma and led to the rather uniform Moho depth of 30 km which still characterizes most of present-day Central Europe (Blundell *et al.* 1992). Thus, when comparing the modelling results to present-day data sets, such as deep seismic reflection profiles, the postcollisional evolution has to be taken into account. In a first approach, this is done by a two-stage transformation process which simulates geometrically postorogenic extension and erosion until a uniform 30km thick crust is obtained. Future work will focus on fully dynamic finite element models covering the whole orogenic evolution by combining the model presented in this paper with models describing postorogenic extension (e.g., Henk 1997).

During the first stage of geometrical transformation, the position of the tracking grid nodes is recalculated assuming constant element areas and a 40% pure shear horizontal extension in the central thickened part of the orogen, decreasing to 0% across two 50 km wide transition zones at the flanks of the orogen. The assumed amount of extension is in correspondence with estimates derived from subsidence analyses of the Saar-Nahe Basin located immediately west of the study area (Henk 1993). Extension already causes a significant decrease in crustal thickness, but to achieve the uniform thickness observed, the remnants of the orogen have to be removed by postconvergent erosion (Fig. 5c). Erosion partly occurred simultaneous with

extension in reality, but is calculated in an individual second step. During this stage, erosion of all material exceeding the reference crustal thickness of 30 km is assumed.

Fig. 6a shows the central part of the tracking grid transformed to the present-day situation, whereas Fig 6b depicts the total von Mises strain accumulated during the convergence stage. Modelling results are compared to a line drawing of deep seismic reflection profiles DEKORP 2N and 2S (Fig. 6c, see Fig. 4 for location) which cross the study area. Both the numerical model and the seismic section show an anomaly within the crustal structure a little more than 100km in width. In the modelled section, it consists of a dome-shaped uplifted lower crust, forming a plateau of deeply-exhumed rocks at the Earth's surface.

The comparison of surface deformation, sandbox experiments and FE models implies, that zones of high cumulative strain in continuum models relate to discrete tectonic structures in nature. Therefore, seismic reflectivity, which is partly created by discrete faults and shear zones, is assumed to correlate with high strain zones within total deformation plots of continuum FE models (Beaumont *et al.* 1994). The position of the domed, outward-verging high strain areas both at the pro- and at the retro-side (Fig. 6b) of the structure resembles the pattern of major reflectors (Fig. 6c) defining the central uplifted structure of the MGCR.

Comparison to petrological data

Another interesting data set are the peak metamorphic pressure and temperature conditions achieved during the Variscan Orogeny. Petrological data published by Anderle *et al.* (1991) for the southernmost Rhenohercynian Zone (pro-wedge), by Willner *et al.* (1991) and Okrusch (1995) for the Odenwald and Spessart Mountains (central pop-up), respectively, and by Schäfer (1997) for the Vesser Zone and the Schwarzburg Anticline (retro-wedge) are used for comparison with the numerical simulation. The maximum pressures and temperatures recorded by the rocks presently at the surface were horizontally projected into a NW-SE trending profile parallel to the DEKORP 2N and 2S traverse (Fig. 4).

Comparison between observed peak metamorphic conditions and calculated maximum pressures and temperatures is shown in Fig. 7. As we want to reproduce P-T data obtained from rocks at the present-day surface, the modeled curves are based on syncollisional peak metamorphic conditions recorded by marker points, which reached the model surface after postcollisional extension and erosion. Field as well as model data show a bell-shaped pressure and temperature profile with plateaus at 6 - 7 kbar and 600 – 650 °C. The overall shape is rather symmetrical and shows only minor differences in the pressure and temperature decrease between pro- and retro-side. However, it should be kept in mind that the uncertainties in thermal parameters and petrologic calibration data also have an influence on the rheological model as crustal strength is strongly temperature-dependent.

Some uncertainties exist concerning the age of the peak metamorphic pressure in the Böllsteiner and Bergsträsser Odenwald (indicated by question marks in Fig. 7a). According to discordant U-Pb age data on zircon of 380 Ma (Todt 1979; Willner *et al.* 1991), pressures of 8 – 10 kbar were already achieved prior to continental collision, i.e. during the preceding subduction stage. In the temperature curve (Fig. 7 b), a major difference between model predictions and observed data from the TKU and NPZ is found. Real peak temperatures are 150-200 °C lower than suggested by the numerical model. This difference is probably related to rapid burial and continuous cooling of these units by underthrusting of cooler rocks as was shown by Henk (1995). This process is related to discrete fault planes and cannot be reproduced by the continuum approach used in the present study.

The numerical model can also be used to predict complete syncollisional P-T paths. Comparison of the contemporaneous P-T evolution of various particle points presently located at the Earth's surface shows systematic variations across the model orogen. Fig. 8 documents six P-T paths from the pro-side (paths 1 to 3) and retro-side (paths 4 to 6) including the time maximum metamorphic conditions were reached after the onset of convergence. The starting point of each path correlates with the conditions in a thermally equilibrated crust as prescribed

by the initial model set-up. In reality, P-T paths will also be influenced by the thermal effects of the precollisional evolution, i.e. subduction of oceanic crust.

Only the three pro-side and the most external retro-side path document an initial prograde evolution as a result of continental collision and burial of rocks, respectively. Decompression on the pro-side starts systematically later with increasing distance from the central block: the most external path shows a longer and more pronounced burial stage, whereas towards the centre of the orogen a short phase of burial is followed by rapid and accelerated exhumation. Consequently, all paths in the pro-wedge area have a clockwise shape with a rather tight loop. The maximum syncollisional exhumation in these parts of the model amounts to about 10 km (path 3). The far retro-side path again resembles pro-side paths with an initial phase of rapid burial, a prolonged period near maximum pressure conditions and some subsequent exhumation. The sample path from the internal part of the retro wedge (path 4) also exhibits significant exhumation of up to 10 km during convergence, but starts with an anticlockwise evolution, i.e. some cooling during initial burial (path 4). The sense of curvature, also in path 5, changes to clockwise after about 10 Ma, contemporaneously with a distinct acceleration in exhumation velocity.

Though a direct reproduction of the observed metamorphic (P-T-t) paths in the study area is not within the scope of this work, there is some good agreement with the model predictions. Very rapid uplift and cooling (as documented by paths 3 and 4) is indicated for the Spessart Mountains by K-Ar dates on hornblendes, muscovites and biotites ranging between 318 and 324 Ma (Okrusch 1995). Counterclockwise stretches (path 4 and 5) show striking similarities with published P-T paths from the Böllsteiner Odenwald (Willner *et al.* 1991) and for the Ruhla Formation of the Ruhla Crystalline Complex (Zeh *in press*).

Conclusions

The general thermo-mechanical models of orogenic evolution presented in the first half of this paper illustrate how crucial the rheology of the lower crust is for crustal thickening and strain localization. If orogens with Moho temperatures in excess of 700 °C are simulated using flow laws commonly applied in geodynamic studies, i.e. anorthosite (Shelton & Tullis 1981) to represent the bulk rheology of the lower crust, models fail to produce significant crustal thickening and strain localization within the crust. Instead, a basal shear zone develops, decoupling deformation in the crust from the mantle, which results in widening of the deformation zone rather than crustal thickening. With respect to petrological data of lower crustal rocks from orogenic settings which often point to Moho temperatures in the range of 700 – 900 °C, this modelling result may indicate that some of the frequently used flow laws are actually too weak. To reproduce observed petrological data and observed orogen geometries a stronger lower crust, with viscosities between 10^{21} – 10^{23} Pa s, is required. This can be achieved, for example, by using a dry diabase rheology (Mackwell *et al.* 1998) to represent the mechanical behaviour of the lower crust.

Application of the numerical model to the collision between two tectonometamorphic units of the Variscan Orogen, the Rhenohercynian and the Saxothuringian Zones, yields quantitative insights into strain partitioning, peak metamorphism as well as the rapid syn-convergent exhumation of metamorphic complexes forming the MGCR.

Observed seismic (DEKORP 2N and 2S) and metamorphic profiles across the MGCR are in good agreement with the presented modelling results, i.e. the orogen's width and geometry after post-convergent extension and erosion. Due to erosion focused on the pro-side (NW) both peak metamorphic temperatures and pressures of rocks presently at the surface show a rather symmetric distribution. The profiles are characterized by a nearly 100km wide

plateau of pressures exceeding 6 kbar and temperatures in the range of 600 to 700°C. Metamorphic temperatures determined for the outcrop areas in distal pro-side position (TKU, NPZ) are distinctly lower than model predictions, which can be explained with cooling of these units by underthrusting of colder rocks. The remaining model predictions agree well with the spatial distribution of peak metamorphic pressure and temperature conditions.

Additionally, numerical simulation results can be used to show systematic variations of contemporaneous pressure-temperature (P-T) paths across the collision zone. Though metamorphic data derived from the MGCR locally show a more complex evolution and there are still uncertainties concerning the exact age of metamorphism, the shape and distribution of model-predicted paths are in first order agreement with their observed petrological equivalents.

This study benefited greatly from discussions with S. Ellis, O. Oncken, E. Stein and A Zeh. C. Beaumont and S. Willett are thanked for their helpful comments on an earlier version of the manuscript. Financial support by the Deutsche Forschungsgemeinschaft as part of the program ‘Orogene Prozesse - ihre Simulation und Quantifizierung am Beispiel der Varisciden‘ is gratefully acknowledged.

References

- ANDERLE, H.-J., MASONNE, H.-J., MEISL, S., ONCKEN, O. & WEBER, K. 1990. Southern Taunus Mountains.. In: FRANKE, W. (ed.), *International conference on paleozoic orogens in Central Europe 1990, field guide "Mid German Crystalline Rise & Rheinisches Schiefergebirge"*, University of Giessen, Giessen, 125-148.
- BEAUMONT, C., FULLSACK, P. & HAMILTON, J. 1994. Styles of crustal deformation in compressional orogens caused by subduction of the underlying lithosphere. *Tectonophysics*, **232**, 119-132.
- BEAUMONT, C. & QUINLAN, G. 1994. A geodynamic framework for interpreting crustal-scale seismic reactivity patterns in compressional orogens. *Geophysical Journal International*, **116**, 754-783.
- BLUNDELL, D., R. FREEMAN, R., and MUELLER, S. 1992. *A continent revealed - The European Geotraverse*, 275 p., Cambridge University Press, London.
- BURG, J.-P., VAN DEN DRIESSCHE, J. & BRUN, J.-P. 1994. Syn- to post-thickening extension in the Variscan Belt of Western Europe: modes and structural consequences, *Géologie de la France*, **3**, 33-51.
- BYERLEE, J.D. 1978. Friction of rocks. *Pure and Applied Geophysics*, **116**, 615-626.
- CERMÁK, V. 1995. A geothermal model of the central segment of the European Geotraverse, *Tectonophysics*, **244**, 51-55.
- DEWEY, J.F. 1988. Extensional collapse of orogens. *Tectonics*, **7**, 1123-1139.
- DITTMAR, D., MEYER, W., ONCKEN, O., SCHIEVENBUSCH, T., WALTER, R. & VON WINTERFELD, C. 1994. Strain partitioning across a fold and thrust belt: the Rhenish Massif, Mid-European Variscides. *Journal of Structural Geology*, **16**, 1335-1352.
- ELLIS, S., BEAUMONT, C., JAMIESON, R.A. & QUINLAN, G. 1998. Continental collision including a weak zone: the vice model and its application to the Newfoundland

- Appalachians. *In*: QUINLAN, G. (ed.), Lithoprobe east transect. *Canadian Journal of Earth Science*, **35**, 11, 1323-1346.
- ENGLAND, P.C. & MOLNAR, P. 1990. Surface uplift, uplift of rocks and exhumation of rocks. *Geology*, **18**, 1173-1177.
- FRANKE, W. 1992. Phanerozoic structures and events in Central Europe. *In*: BLUNDELL, D., FREEMAN, R. & MUELLER, S. (eds.), *A continent revealed - The European Geotraverse*, Cambridge University Press, Cambridge, 164-180.
- HANSEN, F.D. & CARTER, N. L. 1983. Semibrittle creep of dry and wet Westerly Granite at 1000 MPa. *Proceedings - Symposium on Rock Mechanics*, **24**, 429-447.
- HENK, A. 1993. Late orogenic basin evolution in the Variscan internides: the Saar-Nahe Basin, southwest Germany. *Tectonophysics*, **223**, 273-290.
- HENK, A. 1995. Late Variscan exhumation histories of the southern Rhenohercynian Zone and western Mid-German Crystalline Rise: results from thermal modelling. *Geologische Rundschau*, **84**, 578-590.
- HENK, A. 1997. Gravitational orogenic collapse vs. plate-boundary stresses: a numerical modelling approach to the Permo-Carboniferous evolution of Central Europe. *Geologische Rundschau*, **86**, 39-55.
- HENK, A. 1998. Thermomechanische Modellrechnungen zur postkonvergenten Krustenreequilibrierung in den Varisciden. *Geotektonische Forschungen*, **90**, 1-124.
- JAMIESON, R.A. 1991. P-T-t paths of collisional orogens. *Geologische Rundschau*, **80**, 321-332.
- JAMIESON, R.A., BEAUMONT, C., FULLSACK, P. & LEE, B. 1998. Barrovian regional metamorphism: Where's the heat? *In*: TRELOAR, P.J. & O'BRIAN, P.J. (eds.) *What Drives Metamorphism and Metamorphic Reactions?* Geological Society, London, Special Publications, **138**, 23-51.
- KEMNITZ, H. 1995. Phyllitic islands in very low grade surroundings – nappes in Thuringia? A

- microanalytical approach on metamorphic phyllosilicates. *Journal of Czech Geological Society*, **40**, **3**, 20-21.
- KOHLSTEDT, D.L., EVANS, B., & MACKWELL, S.J. 1995. Strength of the lithosphere: constraints imposed by laboratory experiments. *Journal of Geophysical Research*, **100**, 17587-17602.
- MACKWELL, S.J., ZIMMERMAN, M.E. & KOHLSTEDT, D.L. 1998. High-temperature deformation of dry diabase with application to tectonics on Venus. *Journal of Geophysical Research*, **103**, 975-984.
- MEISSNER, R. & BORTFELD, R.K. 1990. *Dekorp-Atlas*, 99 p., Springer-Verlag, Berlin.
- OKRUSCH, M. 1995. Mid-German Crystalline High - Metamorphic evolution. In: DALLMEYER, R.D., FRANKE, W. & Weber, K. (eds.), *Pre-Permian Geology of Central and Eastern Europe*, Springer-Verlag, Berlin, 201-213.
- ONCKEN, O. 1997. Transformation of a magmatic arc and an orogenic root during oblique collision and its consequences for the evolution of the European Variscides (Mid-German Crystalline Rise). *Geologische Rundschau*, **86**, 2-20.
- ONCKEN, O. 1998. orogenic mass transfer and reflection seismic patterns – evidence from DEKORP sections across the European Variscides (central Germany). *Tectonophysics*, **286**, 47-61.
- SCHÄFER, F. 1997. Krustenbilanzierung eines variscischen Retrokeils im Saxothuringikum. *Scientific Technical Report Geoforschungszentrum Potsdam*, **97/16**, 1-131.
- SHELTON, G. and TULLIS, J. 1981. Experimental flow laws for crustal rocks, *EOS*, **62**, 396.
- SUMMERFIELD, M.A. & HULTON N.J. 1994. Natural controls of fluvial denudation rates in major world drainage basins. *Journal of Geophysical Research*, **99**, 13871-13883.
- TODT, W. 1979. U-Pb-Datierungen an Zirkonen des kristallinen Odenwaldes. *Fortschritte der Mineralogie*, **57** (Beiheft 1), 153-154.
- VAUCHEZ, A., TOMMASI, A., BARUOL, G. 1998. Rheological heterogeneity, mechanical

- anisotropy and deformation of the continental lithosphere. *Tectonophysics*, **296**, 61-86.
- WALTER, R. 1992. *Geologie von Mitteleuropa*, 561 p., Schweizerbart'sche Verlagsbuchhandlung, Stuttgart.
- WILLNER, A.P., MASONNE, H.-J. & KROHE, A. 1991. Tectonothermal evolution of a part of a Variscan magmatic arc: the Odenwald in the Mid-German Crystalline Rise. *Geologische Rundschau*, **80**, 369-389.
- WILLETT, S., BEAUMONT, C. & FULLSACK, P. 1993. Mechanical model for the tectonics of doubly vergent compressional orogens. *Geology*, **21**, 371-374.
- ZIEGLER, P.A. 1990. *Geological Atlas of Western and Central Europe*, 239 p., Shell Internationale Petroleum Maatschappij, The Hague.
- ZEH, A., COSCA, M.A., BRAETZ, H., OKRUSCH, M. & TICHOMIROVA, M. (in press). Simultaneous horst-basin formation and magmatism during Late Variscan Transtension: Evidence from $^{40}\text{Ar}/^{39}\text{Ar}$ and $^{207}\text{Pb}/^{206}\text{Pb}$ geochronology in the Ruhla Crystalline Complex. *Geologische Rundschau*.
- ZOTH, G. & HÄNEL, R. 1988. Appendix. In: HÄNEL, R., RYBACH, L. & STEGENA, L. (eds.), *Handbook of terrestrial heatflow density determination*. Kluwer, Dordrecht, 449-466.

Fig. 1. Modelling concept (simplified after Willett *et al.* 1993). **(a)** The initial model set-up describes collision of two continental fragments by applying displacement to the base of one crustal block, while the base of the other is fixed horizontally. The point, where the discontinuity in the basal boundary condition occurs, is termed S and represents the locus of asymmetric detachment and underthrusting of the mantle lithosphere. **(b)** Deformation starts with block uplift between two conjugate deformation zones. **(c)** Continuing convergence leads to formation of a pro-wedge with minimum critical taper and a retro-wedge comprising two segments with maximum and minimum critical taper.

Fig. 2. Deformed finite-element models contoured for total von Mises strain after 100 km of convergence at 20 mm a^{-1} . **(a)** “Cold” crust with an initial Moho temperature of 500°C . For the lower crust the anorthosite flow law of Shelton & Tullis (1981) is assumed. **(b)** “Hot” crust with an initial Moho temperature of 700°C . For the lower crust the anorthosite flow law of Shelton & Tullis (1981) is assumed. **(c)** Same as b but for the lower crust the dry diabase flow law of Mackwell *et al.* (1998) is used.

Fig. 3. Flow laws based on power-law creep parameters of upper and lower crustal rocks (for $\dot{\gamma} = 10^{-14} \text{ s}^{-1}$).

Fig. 4. Sketch map showing Variscan Massifs in Central Europe and the location of the study area. Heavy lines indicate deep seismic reflection profiles used for comparison with the results of the numerical simulations.

Fig. 5. (a) Initial tracking grid (only central part is shown). (b) Deformed tracking grid after the end of convergence. Shading shows the compositional layering within the crust. (c) Total von Mises strain accumulated during the convergence stage. (d) Deformed FE grid geometrically corrected for postconvergent extension and erosion to allow comparison with the present-day crustal configuration. Box indicates central part of the model shown in detail in Fig. 6.

Fig. 6. (a) Deformed FE grid (detail of Fig. 5 c). (b) Total strain accumulated during the convergence stage. (c) Line drawing of deep seismic reflection profiles DEKORP 2N and 2S (after Oncken 1998; see Fig. 4 for location)

Fig. 7. Comparison of modelled peak metamorphic pressures (a) and temperatures (b) presently at surface with observed petrological data along a NW-SE trending profile across the collision zone (abbreviations: TKU – Taunuskamm Unit, NPZ – Northern Phyllite Zone, SPM – Spessart Mountains, OBÖ – Böllsteiner Odenwald, OBS – Bergsträsser Odenwald, VZ – Vesser Zone and SBA – Schwarzburg Anticline; data after Anderle *et al.* 1990, Willner *et al.* 1991; Okrusch 1995; Schäfer 1997).

Fig. 8. Variation of contemporaneous P-T paths for selected points presently at the Earth's surface across the modeled collision zone. Circled numbers indicate the time after the onset of continental collision in Ma. For comparison, schematic P-T paths from the MGCR are given at the top and at the bottom.

Table 1. *Thermal and mechanical material parameters used in this study; whenever possible, material parameters specific to the Variscan Crust in Central Europe are used*

Initial Model Geometry			
thickness upper crust (m)	h_{uc}	15×10^3	
thickness lower crust (m)	h_{lc}	15×10^3	
model width (m)	w_{ini}	1200×10^3	
rate of convergence ($m a^{-1}$)	v_c	15×10^{-3}	
Mechanical Material Properties			
Poisson's ratio	?	0.25	
Upper Crust			
density at 273 °K ($kg m^{-3}$)	?	2800	
Young's Modulus (Pa)	E	0.5×10^{11}	
strain rate coefficient ($Pa^{-n} s^{-1}$)	a_0	3.16×10^{-26}	<i>Hansen & Carter 1983</i>
activation constant (°K)	Q/R	22432	<i>Hansen & Carter 1983</i>
power law stress exponent	n	3.3	<i>Hansen & Carter 1983</i>
bulk strain rate (s^{-1})	?'	1×10^{-14}	
Lower Crust			
density at 273 °K ($kg m^{-3}$)	?	3000	
Young's Modulus (Pa)	E	0.8×10^{11}	
strain rate coefficient ($Pa^{-n} s^{-1}$)	a_0	5.05×10^{-28}	<i>Mackwell et al. 1998</i>
activation constant (°K)	Q/R	58693	<i>Mackwell et al. 1998</i>
power law stress exponent	n	4.7	<i>Mackwell et al. 1998</i>
bulk strain rate (s^{-1})	?'	1×10^{-14}	
Thermal Material Properties			
surface temperature (°K)	T_s	273	
basal heat flow ($W m^{-2}$)	q	0.04	
Upper Crust			
thermal conductivity ($W m^{-1} °K^{-1}$)	k	3 - 1.3	(1), <i>Zoth and Hänel 1988</i>
specific heat ($m^2 s^{-2} °K^{-1}$)	C	1.3×10^3	
radiogenic heat production ($W m^{-3}$)	H	2.3×10^{-6}	(2), <i>Cermák 1995</i>
Lower Crust			
thermal conductivity ($W m^{-1} °K^{-1}$)	k	2.5 - 1.7	(1), <i>Zoth and Hänel 1988</i>
specific heat ($m^2 s^{-2} °K^{-1}$)	C	1.3×10^3	
radiogenic heat production ($W m^{-3}$)	H	0.52×10^{-6}	(2), <i>Cermák 1995</i>

(1) temperature-dependent

(2) corrected for 300 Ma

Fig. 1

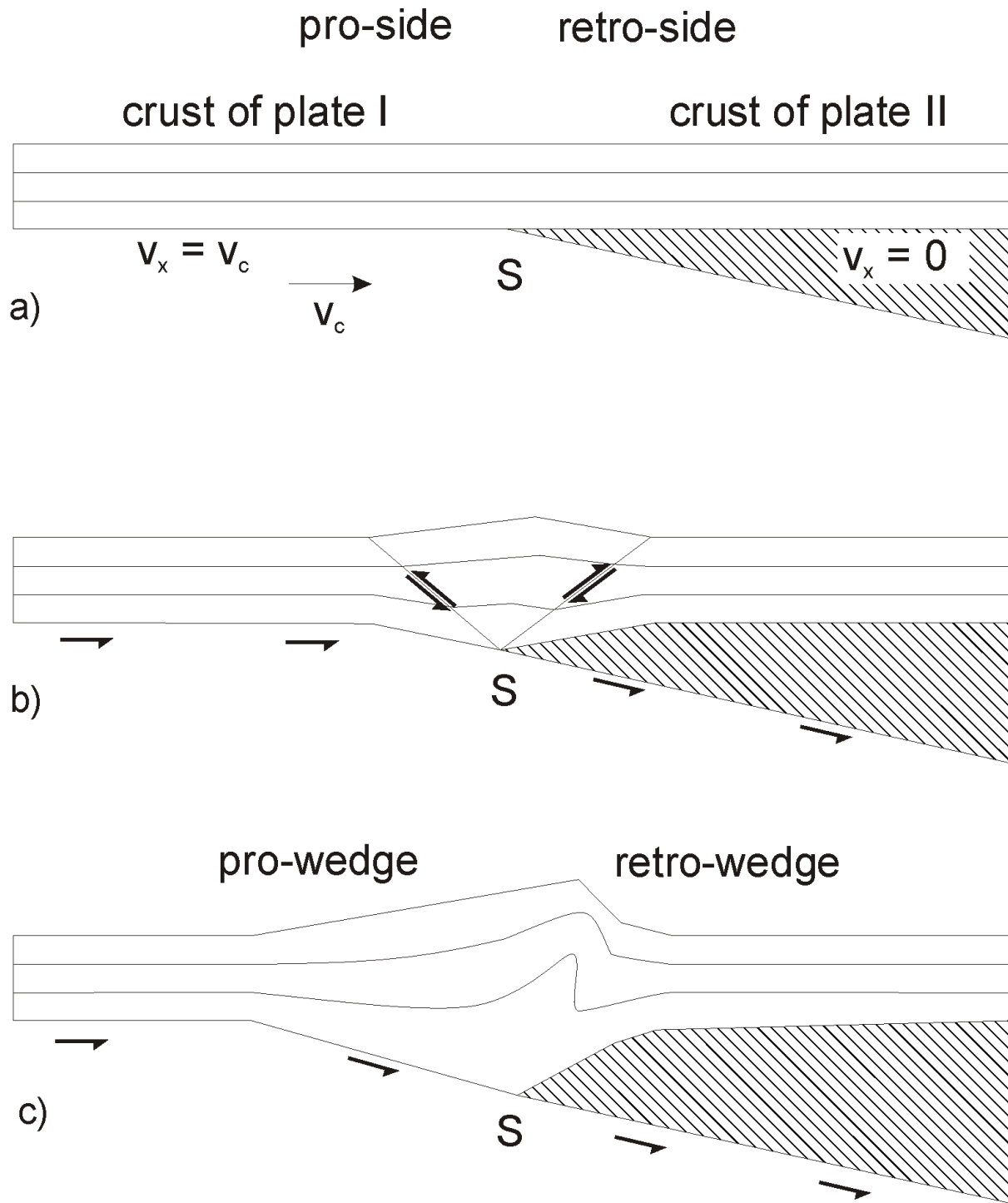


Fig. 2

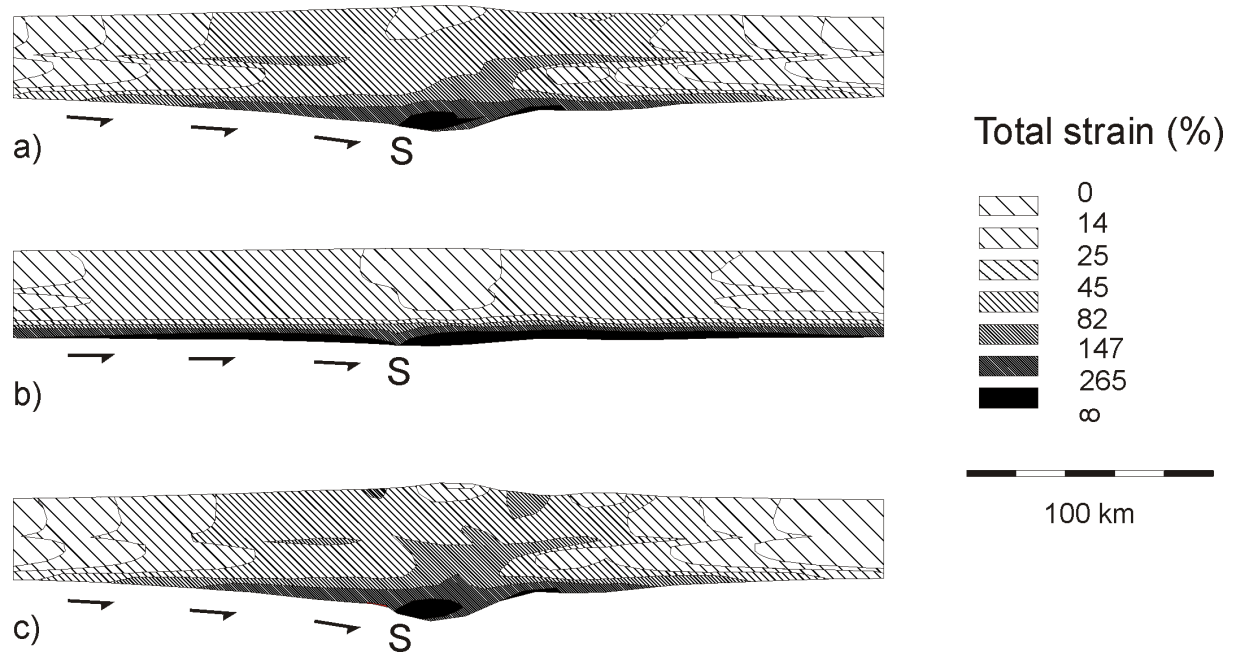
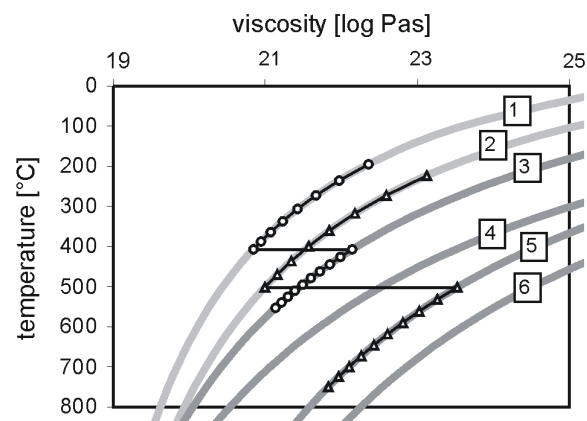


Fig. 3



- 1 Paterson & Luan (1990): Wet Quartzite
- 2 Hansen & Carter (1983): Dry Westerly Granite
- 3 Shelton Tullis (1981): Dry Anorthosite
- 4 Wilks & Carter (1990): Mafic (Pikwitonei) Granulite
- 5 Mackwell et al. (1998): Dry Maryland Diabase
- 6 Boutilier & Keen (1994): "Standard Model"
- Flow laws used in figures 2a and b
- ▲ Flow laws used in all other figures

Fig. 4

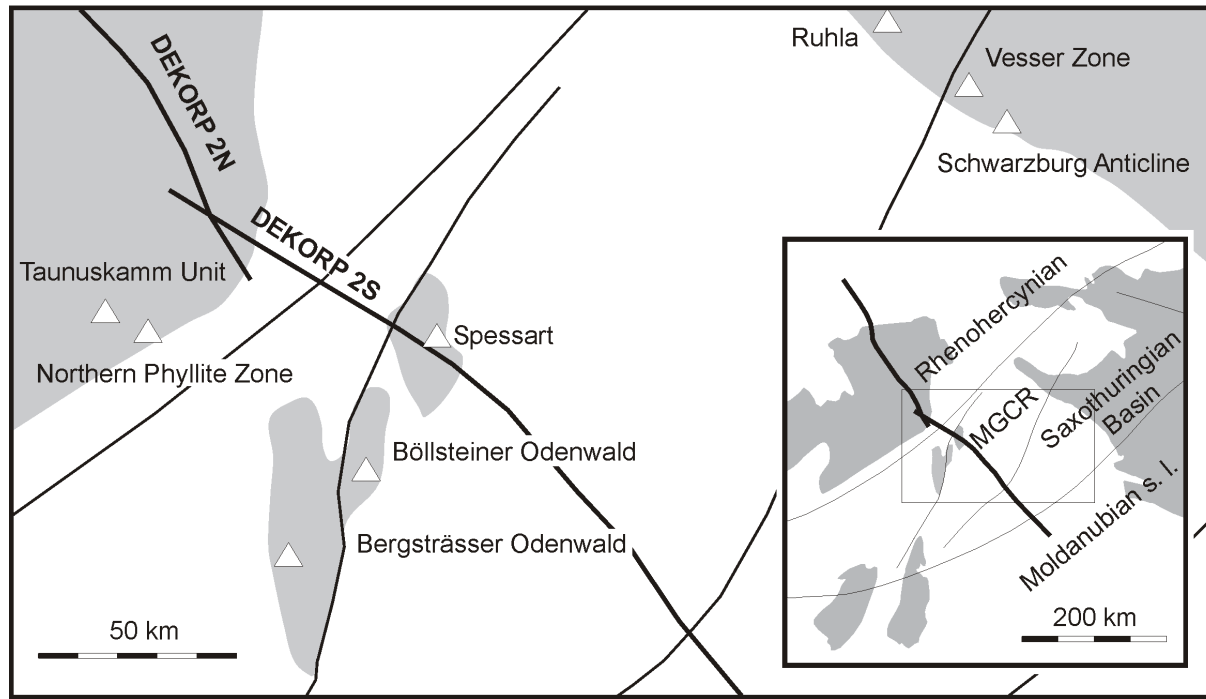
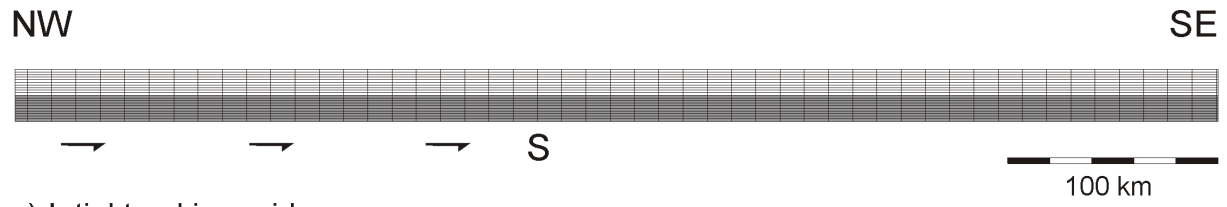
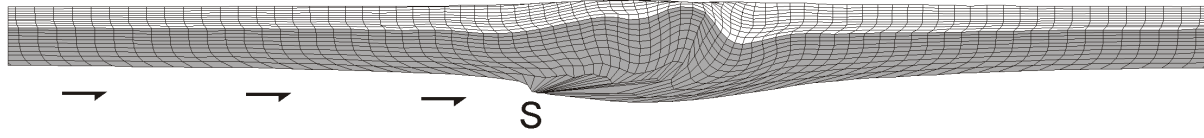


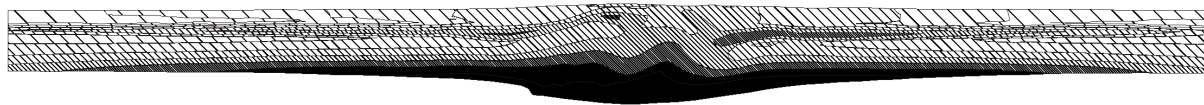
Fig. 5



a) Initial tracking grid

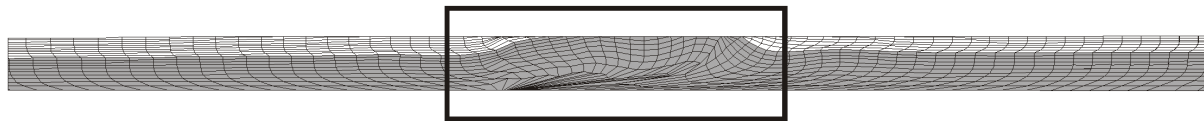


b) Deformed tracking grid



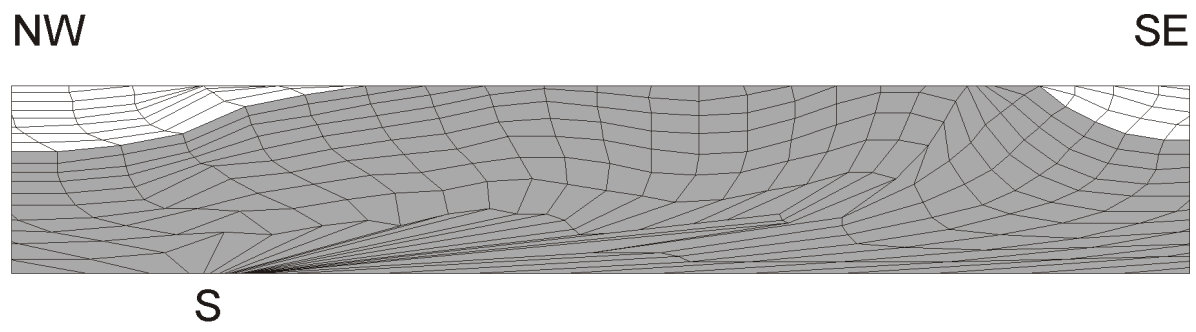
0  14  25  45  82  147  265  476  857  ∞

c) Total strain (%) accumulated during convergence

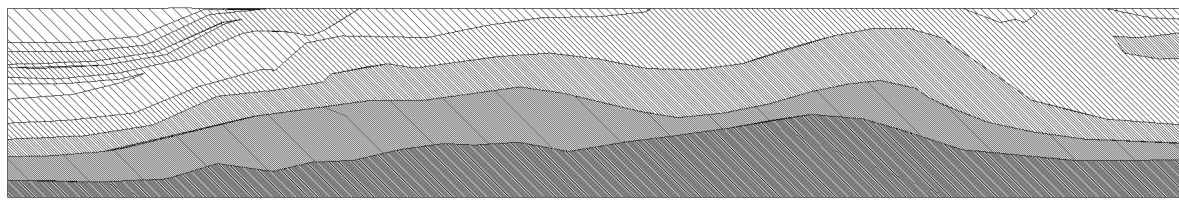


d) Grid restored for postconvergent extension and erosion

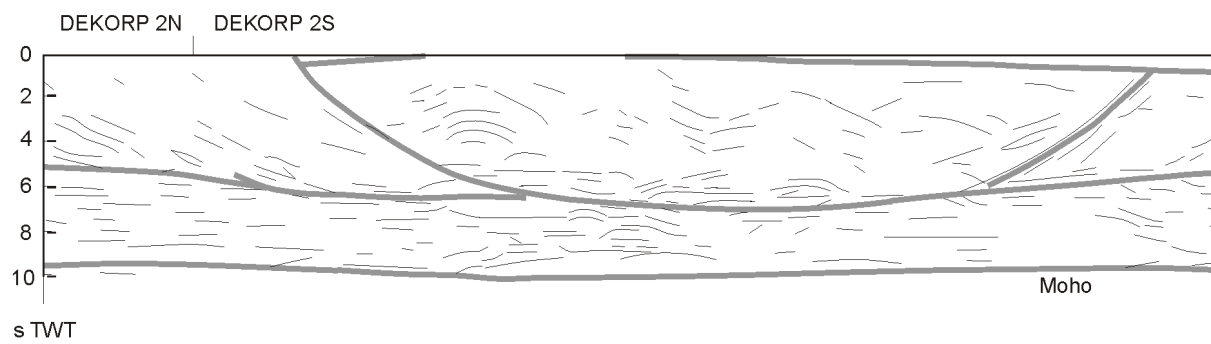
Fig. 6



a) Grid restored for postconvergent extension and erosion



b) Total strain (%) accumulated during convergence



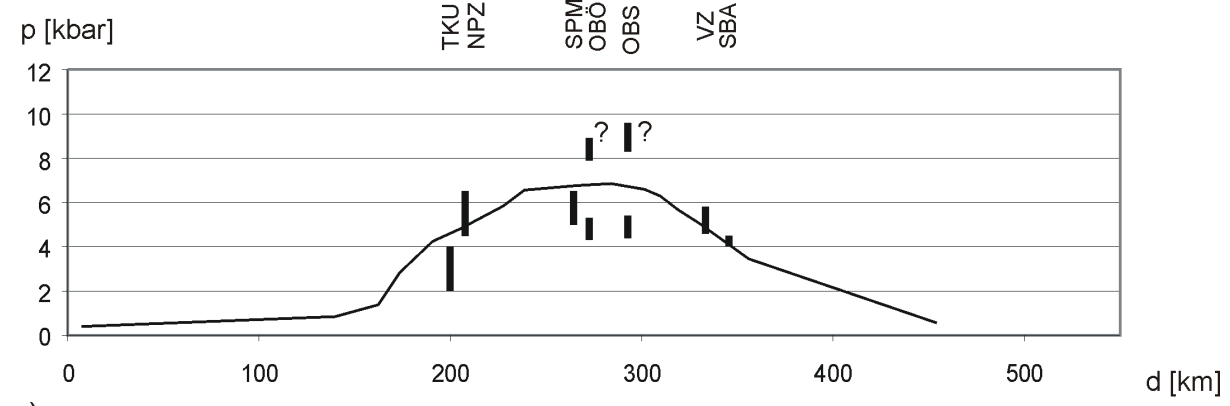
c) Line drawing

50 km

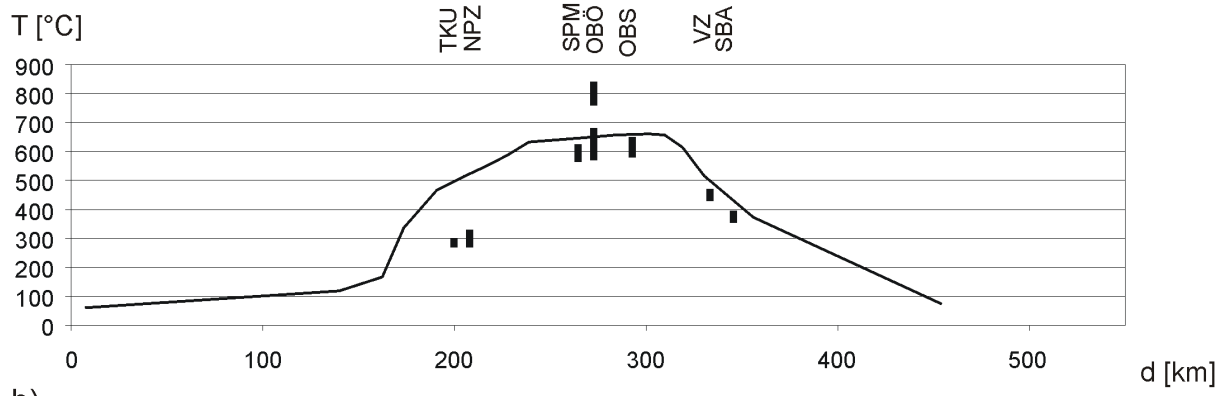
Fig. 7

NW

SE



a)



b)

Fig. 8

